AJNR Am J Neuroradiol 19:943–950, May 1998

Near-Resonance Saturation Pulse Imaging of the Extraocular Muscles in Thyroid-Related Ophthalmopathy

John L. Ulmer, Sangeeta C. Logani, Leighton P. Mark, Craig A. Hamilton, Robert W. Prost, and James N. Garman

PURPOSE: **We examined the utility of near-resonance saturation pulse imaging (magnetization transfer [MT] and spin lock) in characterizing microstructural changes occurring in the extraocular muscles of patients with thyroid-related ophthalmopathy (TRO).**

METHODS: **Eight healthy volunteers and 10 patients with TRO were imaged using an off-resonance saturation pulse in conjunction with conventional spin-echo T1-weighted imaging at frequency offsets of 500, 1000, 1500, and 2000 Hz from water resonance. The relative contributions of MT and spin-lock excitation to image contrast at each frequency offset were estimated using a computer simulation model. Suppression ratios were calculated for the control and TRO groups from measurements obtained on two successive coronal sections in the widest portion of the inferior and medial rectus muscles bilaterally. A repeated measures analysis of variance and a parametric correlation analysis were performed to evaluate maximum cross-sectional area, MR-generated signal, and suppression ratios for the extraocular muscles examined.**

RESULTS: **Our computer model suggested that saturation of extraocular muscles was due to pure MT effects with our off-resonance pulse at 2000 and 1500 Hz, to a combination of MT and spin lock at 1000 Hz frequency offset, and, primarily, to spin-lock excitation at 500 Hz frequency offset. Suppression ratios for the extraocular muscles of the TRO patients were significantly lower than that observed for the control subjects at 1500, 1000, and 500 Hz frequency offset. This differential saturation effect was maximal at 500 Hz frequency offset, with mean suppression ratios for the inferior and medial rectus muscles of 27% for the healthy subjects and 20% for the TRO group.**

CONCLUSION: **Both MT and spin-lock contrast of the extraocular muscles in patients with TRO differ significantly from that observed in control subjects. Near-resonance saturation pulse imaging may enhance our understanding of the microstructural changes occurring in the extraocular muscles of these patients.**

Thyroid-related ophthalmopathy (TRO), otherwise known as Graves' ophthalmopathy, is an immune-mediated inflammatory disorder of the orbital tissues found in conjunction with thyroid disease, commonly affecting the extraocular muscles (1–3). The diagnosis of TRO may be straightforward or may present a diagnostic dilemma. The combination of bilateral proptosis, lid retraction, and enlarged thyroid are virtually pathognomonic for TRO. While 75% of patients have characteristic findings of Graves' ophthalmopathy, a significant proportion may have no hyperthyroidism or only marginal orbital symptoms, making the diagnosis difficult. In most patients, orbital disease occurs within 18 months before or after the onset of clinical hyperthyroidism. However, thyroid dysfunction and orbital disease can be separated by months to years in some cases. Extraocular muscle involvement may be present in patients with Graves' disease who have no orbital signs or symptoms. Other patients may show signs and symptoms of orbital inflammation without evidence of extraocular muscle enlargement. Although the inferior and medial recti are most commonly affected, extraocular muscle disease may be asymmetric, involving any of the muscles

Received June 24, 1997; accepted after revision October 29.

From the Departments of Radiology (J.L.U., L.P.M., R.W.P., J.N.G.) and Ophthalmology (S.C.L.), Medical College of Wisconsin, Milwaukee, and the Department of Radiology, Bowman Gray School of Medicine, Winston-Salem, NC (C.A.H.).

Address reprint requests to John L. Ulmer, MD, Department of Radiology, Medical College of Wisconsin, Froedtert Memorial Lutheran Hospital, 9200 W Wisconsin Ave, Milwaukee, WI 53226.

in one or both orbits. Thus, characterizing TRO on the basis of clinical criteria can be difficult, and a variety of ancillary tests may be required to support the diagnosis.

As a consequence of the protean nature of TRO, identification of the various histologic phases within the extraocular muscles is difficult. Because of the inherent morbidity associated with a biopsy of such a small structure, the routine use of tissue specimen analysis on an individual basis is impractical. At the same time, histologic determination of this sort would be useful in selecting treatment options. For example, steroid and radiation therapy are most effective during the acute (inflammatory) stages of the disease. Myopathic restriction, on the other hand, is presumably related to deposition of fibrotic tissue. Muscle enlargement resulting in proptosis and optic neuropathy is likely multifactorial and may relate to inflammation, edema, and/or the accumulation of fatty tissue. In short, the histologic changes within the extraocular muscles of patients with TRO are difficult to characterize and may occur at different stages within individual muscles or different muscles within individual patients. To date, there is no noninvasive method used routinely in clinical practice to evaluate tissue structural changes in these patients.

Off-resonance saturation imaging is a recently developed MR imaging technique that selectively alters contrast on the basis of tissue macromolecular environments (4–6). The technique uses preparatory RF radiation in conjunction with standard imaging sequences to effect local magnetic processes responsible for tissue discrimination in MR imaging. The potential for off-resonance saturation imaging to improve visual contrast and to obtain quantitative information from normal and pathologic tissues in the brain and extracranial head and neck is a subject currently under extensive investigation (6–16). Studies suggest that an off-resonance preparatory pulse applied 2000 Hz or more from water resonance achieves tissue saturation indirectly by a mechanism known as magnetization transfer (MT) (4). However, as the preparatory pulse is brought closer to water resonance, a direct saturation mechanism known as spin lock contributes to image contrast (5, 6). While MT alters tissue contrast on the basis of intermolecular interactions, reflecting transfer of energy from hydrophilic macromolecules to tissue water, near-resonance spin-lock saturation is directly dependent on the T1 and T2 relaxation times of the substance imaged. The same environmental factors that produce strong MT effects in a given tissue also contribute to spin-lock effects, but these processes are distinct and their ability to alter image contrast may differ significantly depending on the tissue type. Thus, the utility of spin-lock imaging in characterizing tissue microstructural changes in pathologic conditions may differ significantly from that observed with pure MT imaging and remains to be investigated.

Normal skeletal muscle has been shown to exhibit strong MT effects (17–19). To date, however, there has been little investigation into the effects of near-resonance spin-lock imaging in pathologic conditions of skeletal muscle, and we have found no reported studies in which near-resonance saturation techniques were used to evaluate the extraocular muscles in pathologic states. The purpose of this investigation was to characterize the effects of off-resonance saturation imaging on the extraocular muscles of healthy subjects and of patients with TRO. Specifically, our goal was to compare image signal suppression achieved in the inferior and medial recti of healthy subjects with that in patients with TRO by applying off-resonance preparatory RF radiation at a range of frequency offsets (500–2000 Hz) expected to produce both MT and spin-lock effects in skeletal muscle. By doing this, we hoped to elucidate the potential utility of these techniques in characterizing microstructural changes in the extraocular muscles of patients with Graves' ophthalmopathy and to determine the saturation pulse-frequency offset required to achieve optimal contrast between healthy and diseased tissue.

Methods

Off-Resonance Saturation Pulse Sequence

MR imaging was performed on a 1.5-T unit. The off-resonance saturation pulse had a bandwidth of approximately 200 Hz. A Fermi pulse was used with a duration of 16 milliseconds and a peak pulse amplitude of 9.7 μT. The saturation pulse was relatively adiabatic in nature with a limited rise and fall time to achieve near-resonance spin-lock effects while avoiding spin-tip excitation (5). After each saturation pulse, gradient homospoiling was performed by turning on the *y*-axis (phase-encoding gradient) to maximum amplitude for about 5 milliseconds. Allowing for gradient ramp times, the interval between the end of the saturation pulse and the beginning of the 90° pulse was approximately 6 milliseconds. The multisection off-resonance saturation pulses are nonselective and their saturation effects are cumulative throughout the repetition time.

Off-resonance saturation pulse T1-weighted imaging with frequency offsets of 500, 1000, 1500, and 2000 Hz from water-resonance was used for both the age-matched healthy volunteers and the patients with TRO. Specific absorption rates were carefully monitored and remained below limits mandated by the Food and Drug Administration (average, 3.2 W/kg for the whole head and 8.0 W/kg for any single gram of tissue). Computer simulations utilizing published T1 (870 milliseconds) and T2 (47 milliseconds) relaxation times for normal skeletal muscle (20) were used to estimate the contribution to signal suppression from near-resonance spin-lock excitation, using modified Bloch equations and a simulation method described in a previous report by Moran and Hamilton (5).

Coronal T1-weighted images were acquired with and without the off-resonance saturation pulse with imaging parameters of 650/31/1 (TR/TE/excitations), 24-cm field of view, 512 × 512 matrix, 3-mm section thickness, 1.5-mm intersection gap, and flow compensation. Imaging time for the T1-weighted spin-echo sequence (six sections) with and without the off-resonance saturation pulse applied was 5 minutes 42 seconds. Patients and volunteers were instructed to focus on a single visual point in the scanner suite to reduce eye motion during the imaging sequences. Receive and transmit attenuator settings were held constant to compare the pulse sequences for each experiment.

Patient Selection

The imaging studies were explained to all subjects, and informed consent was obtained. The off-resonance saturation

sequences were tested in eight healthy volunteers who reported no history of orbital abnormalities or thyroid dysfunction. Volunteers (four men and four women) ranged in age from 36 to 63 years (mean, 51 years). Ten patients with TRO diagnosed at the eye institute of our institution were enrolled in the study. All had orbital symptoms and supportive laboratory data to establish the diagnosis. The group ranged in age from 42 to 72 years (mean, 56 years) and included four men and six women. At the time of the study, none of the patients were being treated with any form of immunosuppressant or radiation therapy.

Tissue Measurements

Quantitative single analysis was performed only in the inferior and medial rectus muscles of each orbit in both the volunteer and TRO groups. Regions of interest were placed at the largest portion of the extraocular muscle belly in both groups on two successive coronal sections. Suppression ratios (see below), maximum cross-sectional diameters, and signal measurements were obtained at these locations. All values obtained from these measurements were then averaged for each muscle (two sections) and the values for the four muscles examined in each subject were then averaged. Thus, a single value for extraocular muscle cross-sectional area, T1-weighted MR signal, and suppression related to the off-resonance saturation pulse was determined for each volunteer and each TRO patient at each frequency offset. A repeated measures analysis of variance was used to compare the means between the two groups at the saturation pulse-frequency offsets used. Parametric (Pearson) correlation analysis of extraocular muscle maximum cross-sectional area, MR signal, and suppression ratios were calculated.

Tissue-Suppression Ratio

Suppression ratios were calculated with the formula

$$1) \qquad SR = (SI_o - SI_s)/SI_o$$

where SR is the suppression ratio, SI_o is the signal intensity of the extraocular muscle tissue before the saturation pulse was applied, and SI_s is the signal intensity after the saturation pulse was applied. Suppression ratios are convenient measures used by investigators (6, 8–12) to quantify the extent of saturation of a given tissue using off-resonance pulse sequences. The suppression ratio indicates the proportion of signal loss that occurred during the saturation experiment, and multiplying the suppression ratio by 100% yields the percentage of signal suppression in a given tissue related to the off-resonance preparatory pulse.

Results

Off-Resonance Pulse Analysis

A computer simulation (5) of the off-resonance saturation pulse used in this investigation suggests that, for our pulse amplitude (9.7 μT), frequency offsets of 1500 and 2000 Hz result in nearly pure MT saturation of skeletal muscle, with less than 2% signal suppression from spin-lock excitation. At 1000 Hz, the simulation suggests that suppression of signal is a result of the combined effects of MT and spin lock. However, at 500 Hz, essentially all of the suppression observed in this investigation could be accounted for by spin-lock mechanisms. The computer simulation suggested that approximately 30% signal suppression could be achieved with our off-resonance pulse at 500 Hz offset in materials having T1 and T2 relaxation times similar to that of normal skeletal muscle (20).

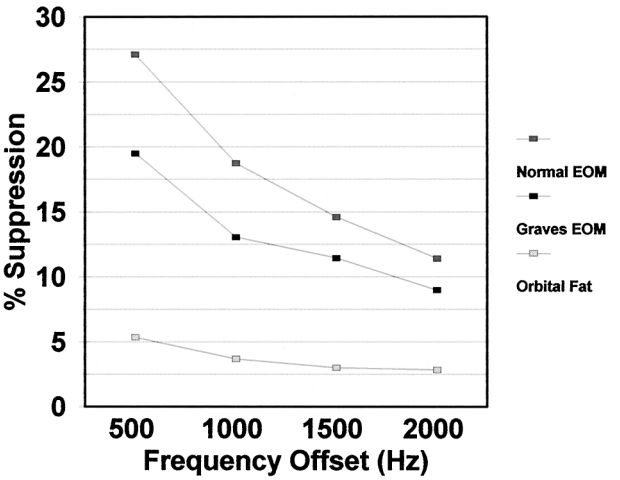

FIG 1. Graph illustrates mean suppression ratios for medial and inferior rectus muscles combined in healthy subjects and in patients with thyroid-related ophthalmopathy (TRO). Extraocular muscles (EOMs) of patients with Graves' disease show significantly lower suppression ratios as compared with healthy control subjects ($P < .01$). Normal orbital fatty tissue shows relatively little signal suppression related to the off-resonance pulse at each of the frequency offsets; EOM fatty infiltration could be one contributing factor to abnormally low EOM signal suppression in the TRO group.

Extraocular muscle suppression ratios in healthy subjects and in patients with thyroid-related (Graves') ophthalmopathy

Healthy Subjects (500 Hz)			Patients with Graves' Disease (500 Hz)		
Patient	Age/ Sex	Suppression Ratio, %*	Patient	Age/ Sex	Suppression Ratio, %*
1	36/M	29.8	1	42/F	18.7
2	36/M	31.5	2	45/F	20.4
3	42/F	34.5	3	47/F†	14.6
4	50/F	24.5	4	52/F	20.7
5	50/F	26.4	5	54/F	22.4
6	60/F	17.5	6	57/F	22.5
7	63/M	23.4	7	60/M	19.5
8	63/M	29.3	8	65/M	25.2
			9	70/M	12.3
			10	72/M	18.6

* Averaged values for inferior and medial recti bilaterally.

† Patient with euthyroid Graves' ophthalmopathy.

Suppression Ratios of Normal Extraocular Muscles

The mean suppression ratios for the medial and inferior rectus muscles of healthy subjects ranged from 27% (± 5.0) at a saturation pulse-frequency offset of 500 Hz to 11% (± 4.9) at a frequency offset of 2000 Hz from water resonance (Fig 1). There was no significant correlation between age of the subjects and calculated extraocular muscle suppression ratios. However, in one 60-year-old woman, suppression ratios at each of the frequency offsets were clearly lower than in the other volunteers (Table), representing

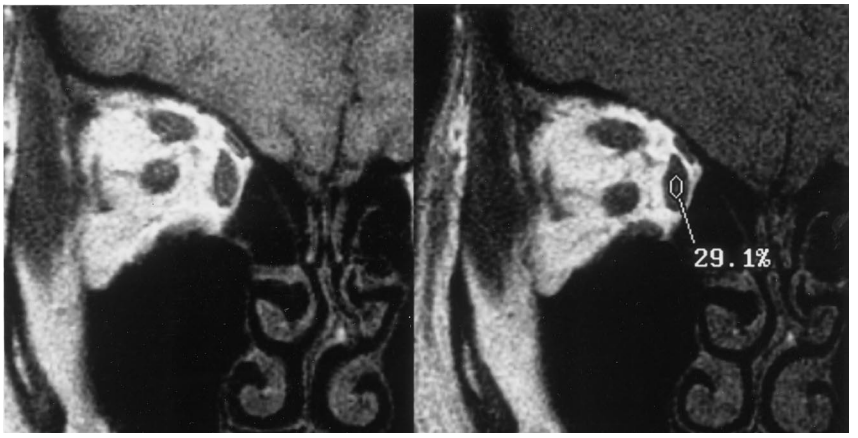

FIG 2. Healthy 50-year-old woman. T1-weighted image without (*left*) and with (*right*) an off-resonance saturation pulse applied at 500 Hz frequency offset. Image on the right shows signal suppression of brain, optic nerve, nasal tissues, temporalis muscle, and extraocular muscles. The medial rectus has a suppression ratio of 29%, a maximum cross-sectional area of 29.3 mm^2, and signal intensity of 249.5. Window width and level settings are constant.

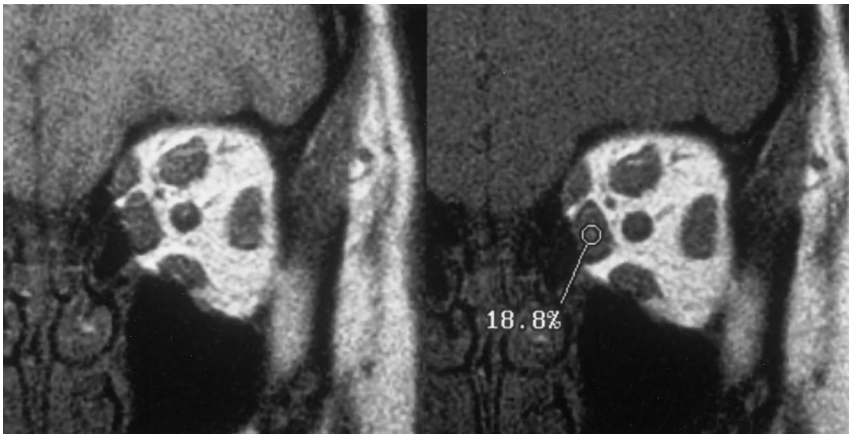

FIG 3. Patient with Graves' disease. T1-weighted image without (*left*) and with (*right*) off-resonance saturation pulse applied at 500 Hz frequency offset. Extraocular muscles are enlarged with reduced signal suppression compared with control subjects (compare with Fig 2). Medial rectus muscle suppression ratio measures 19%. Window width and level settings are constant.

outlying data points. There was a nonsignificant trend toward reduced suppression ratios for the inferior rectus muscles compared with the medial rectus muscles in healthy subjects, which may reflect partial volume effects of adjacent orbital fat. Sampling of normal orbital fat resulted in suppression ratios ranging from 5% (± 4.1) at 500 Hz frequency offset to 3% (± 3.7) at 2000 Hz frequency offset (Fig 1).

Extraocular Muscles of Thyroid-Related Ophthalmopathy

Mean suppression ratios calculated for inferior and medial rectus muscles in patients with TRO ranged from 20% (± 3.6) at a saturation pulse-frequency offset of 500 Hz to 9% (± 4.0) at 2000 Hz frequency offset. As a group, the suppression ratios in the inferior and medial rectus muscles of TRO patients were significantly lower than that observed in healthy subjects ($P < .01$) (Figs 1, 2, and 3). At the individual frequency offsets, suppression ratios were significantly lower at 1500 Hz, 1000 Hz, and 500 Hz than were those observed in the healthy subjects at corresponding frequency offsets. The difference in signal suppression for inferior and medial rectus muscles between the TRO and control groups increased as the frequency offset was decreased toward water resonance, indicating optimal contrast between the two groups in the near 500 Hz range (Fig 1). There was a nonsignificant trend toward reduced suppression ratios for the inferior rectus muscles compared with the medial rectus muscles in the TRO group, which may reflect greater frequency or severity of disease involvement in the inferior recti. The mean suppression ratios at each of the frequency offsets in orbital fat of patients with TRO ranged from 6% (± 2.4) at 500 Hz frequency offset to 3% (± 2.5) at 2000 Hz frequency offset, showing no significant difference as compared with the control group. There was no significant correlation between patients' age and extraocular muscle suppression ratios.

The maximum cross-sectional areas of the extraocular muscles sampled were significantly greater for the TRO group than for the volunteers ($P < .01$) (Figs 2 and 3), with the inferior rectus muscles showing mean cross-sectional diameters of 47.8 mm (± 20.0) compared with 27.9 mm (± 6.3), and for the medial rectus, 58.4 mm (± 30.3) compared with 21.2 mm (± 7.3) in the TRO and control groups, respectively. However, there was considerable overlap between the two groups, with a significant proportion of TRO patients having grossly normal extraocular muscle size despite the presence of other clinical and laboratory findings of Graves' ophthalmopathy. While most of the patients with abnormally low extraocular muscle suppression ratios had enlarged muscles, there was no significant correlation between

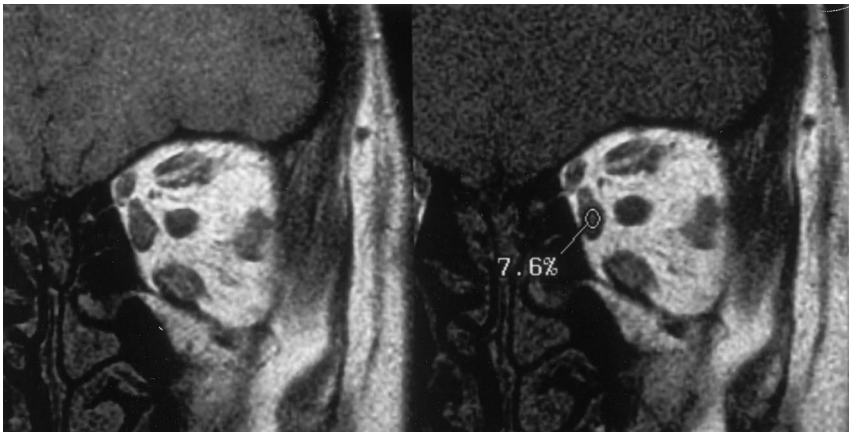

FIG 4. Patient with euthyroid Graves' ophthalmopathy. T1-weighted image without (*left*) and with (*right*) off-resonance saturation pulse applied at 500 Hz frequency offset. Medial rectus muscle shows very little (7.6%) signal suppression. Comparison with Figure 2 reveals medial rectus size and signal similar to healthy control subject, but with grossly abnormal suppression related to the near-resonance saturation pulse. Maximum cross-sectional area is 26 mm^2 and MR signal is 257.5. Window width and level settings are constant.

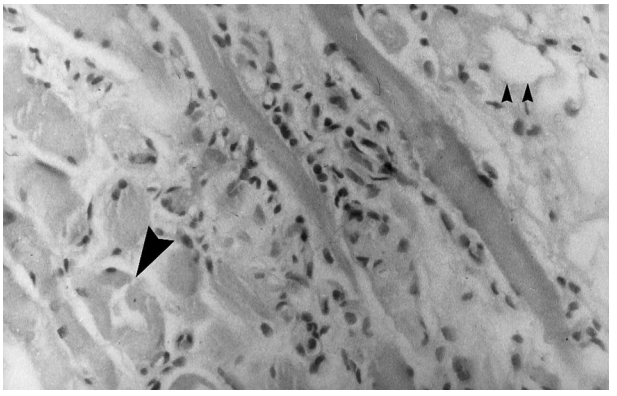

FIG 5. Pathologic specimen of inferior rectus muscle from 60-year-old patient with Graves' disease. Interfibrillar (endomysial) mucopolysaccharide, inflammatory cells, fibrosis, fatty degeneration (*small arrowheads*), and atrophic muscle bundles (*large arrowhead*) are seen. Suppression ratio at 500 Hz frequency offset for this muscle before biopsy was 19%.

these parameters. Many patients with normal-sized muscles also had abnormal suppression ratios (Fig 4).

There was a nonsignificant trend toward increased T1-weighted MR signal of the extraocular muscles in the TRO group (273.4 ± 41.9) compared with the healthy control subjects (247.0 ± 18.3), although there was a significant overlap in signal between the two groups. Visible fatty infiltration of enlarged extraocular muscles was only seen in a small minority of TRO patients. Of the patients with abnormally low signal suppression, many had clearly normal extraocular muscle MR signal (Fig 4). There was no significant correlation between extraocular muscle MR signal and suppression ratios, although a nonsignificant trend was observed at 500 Hz ($r = -.58$).

Nine of the 10 patients with TRO had clinical evidence of hyperthyroidism (Table). One patient who was euthyroid with classic clinical signs and symptoms of TRO had dramatically decreased suppression ratios of all the muscles sampled despite normal medial rectus muscle size and signal (Table) (Fig 4). One 60-year-old man with TRO underwent extraocular muscle biopsy at the time of surgical decompression (Fig 5).

Discussion

Thyroid-related ophthalmopathy (TRO), or Graves' ophthalmopathy, is a disorder of the orbital tissues, usually found in conjunction with immune-mediated thyroid disease (1–3). Of those patients with TRO, approximately 85% have laboratory evidence of Graves' hyperthyroidism. The remaining minority of patients have Hashimoto's thyroiditis, primary hypothyroidism, or are euthyroid in nature. Thus, the diagnosis of TRO may or may not be associated with classic systemic findings of thyroid dysfunction (1–3). Patients without typical biomedical abnormalities but with signs of TRO are considered to have euthyroid Graves' ophthalmopathy. Many of these patients may have other laboratory abnormalities, suggesting autoimmune thyroid disease, including anti–thyroid-stimulating hormone receptor antibodies, but a subset will have no such findings at the time of diagnosis despite typical clinical signs of TRO. This latter subcategory of patients often present a diagnostic dilemma to ophthalmologists and oculoplastic surgeons, particularly before gross extraocular muscle enlargement occurs.

Even patients in whom classic Graves' ophthalmopathy ultimately develops can have an atypical onset of presentation (3). Classically, patients present with thyroid dysfunction and orbital changes within 18 months of each other. However, thyroid and orbital disease can be separated by years, making the diagnosis of TRO uncertain in patients without classic findings. In this setting, imaging techniques may yield important ancillary information in establishing the diagnosis of TRO, but may also be nondiagnostic early in the disease course. At the same time, early diagnosis of TRO is important in the decision to initiate specific immunosuppressant therapies, which are most effective during the acute phases of the disease (3).

The histopathology of extraocular muscle disease in Graves' ophthalmopathy has been investigated (21–23). Proptosis is a result of an increased orbital content, most notably enlarged extraocular muscles. In the acute phases of the disease, extraocular muscles may be grossly enlarged due to inflammation and edema, with associated infiltration of inflammatory

cells in the endomysial tissues, including lymphocytes, neutrophils, and plasma cells. With progression of the disease, there is fibroblastic proliferation and deposition of mucopolysaccharide ground substance. In more chronic stages, collagen deposition results in fibrosis and associated fat accumulation, also primarily between atrophied extraocular muscle fibers. While the general progression of histopathologic changes of TRO has been suggested, the predilection of the disease to affect muscles asymmetrically and at different times during the disease process makes a certain histologic classification in any individual patient difficult. Additionally, the potential morbidity of biopsy makes histologic sampling of the extraocular muscles clinically impractical.

A variety of computed cross-sectional imaging techniques has been used to characterize and evaluate the extraocular muscles in patients with TRO, including CT, sonography, and MR imaging (24–30). However, these imaging methods are largely limited to analysis of extraocular muscle morphology. Recent investigations suggest that sonography is superior to CT for estimating extraocular muscle size in patients with TRO and may reveal irregularities in tissue reflectivity, indicating tissue heterogeneity (24, 26). MR imaging is a useful method for discriminating the soft tissues of the orbit, although it is limited by its poor delineation of bone, and establishing the diagnosis of compressive optic neuropathy at the bony apex may be difficult. Recently, MR imaging techniques have been developed to characterize orbital Graves' disease activity in which measurements of T2 relaxation times and signal on short-inversion-time inversion recovery (STIR) sequences are used to detect the presence of edema related to extraocular muscle inflammation (27–29). These studies suggest that such pulse sequences may be useful in identifying patients who are likely to respond to steroid and radiation therapy. However, measuring T2 relaxation times is a cumbersome technique that is not practical for clinical neuroimaging, and increased signal on STIR sequences related to inflammation and edema might only be present in the most acute phases of the disease. Thus, current imaging techniques are limited in the evaluation of histologic changes associated with TRO.

Off-resonance saturation pulse imaging is a relatively new MR imaging technique that selectively alters the contrast of tissues on the basis of macromolecular, or structural, environments. To accomplish this, a preparatory pulse of low amplitude and short duration is applied to a specific frequency offset from water resonance before a conventional imaging sequence is performed. Although standard off-resonance pulse sequences are now commercially available, the optimal pulse parameters for given pathologic conditions have not been fully explored. If the off-resonance pulse, in the range of amplitudes currently used in clinical brain imaging, is kept at least 2000 Hz from water resonance, the saturation effect is modulated by the process of MT (4). In MT imaging, selective saturation of short T2 species associated with immobile hydrophilic macromolecules is transferred to imagable protons by dipolar coupling mechanisms. However, as the frequency offset is brought closer to water resonance, direct saturation effects may occur that do not require the presence of hydrophilic macromolecules (5, 6, 31–33). Recent investigations (5, 6) suggest that these non-MT near-resonance saturation effects can be explained on the basis of spin-lock excitation, provided the saturation pulse is near adiabatic in design with a gradual rise and fall time. The clinical utility of near-resonance spin-lock imaging has yet to be fully determined.

In spin-lock imaging, tissue contrast is altered by exploiting an effective relaxation time known as $T1_\rho$ in a rotating frame of reference (34–36). The degree of saturation achieved with spin-lock imaging is highly sensitive to the frequency offset of the RF pulse. With frequency offsets far removed from water resonance, $T1\rho$ will approach T1 relaxation time. However, as the frequency offset is brought closer to water resonance, the magnetization relaxes more rapidly toward a new, smaller equilibrium, resulting in suppression of MR image signal. The degree of spin-lock saturation achieved in a given material is dependent on the T1 and T2 relaxation time of that substance, which is in turn dependent on the concentration of hydrophilic macromolecules that modulate free-water relaxivity. Like MT, water protons interacting with macromolecules are susceptible to spin locking, but these phenomena act by different mechanisms and at different frequency offsets.

Several investigations have used spin-lock techniques to suppress tissue selectively and to improve visual contrast between normal structures and abnormal lesions, including in vitro and in vivo breast lesions and tumors containing paramagnetic substances in mice (34–36). The findings in one recent investigation (6) suggest that near-resonance spin-lock imaging is superior to MT in optimizing contrast of enhancing CNS lesions. However, near-resonance spin-lock contrast has not been used to characterize the extraocular muscles in normal and pathologic conditions. If one assumes that spin-lock excitation in tissues is similar to that of semisolid phantom materials (5), computer simulations used in this investigation suggest that skeletal muscle should exhibit strong spin-lock saturation on the basis of published T1 and T2 relaxation times (20). This assumption may or may not be valid. Nevertheless, our simulations suggest that at 500 Hz frequency offset, for our pulse amplitude, most of the extraocular muscle signal suppression observed in this investigation could be accounted for by spin-lock mechanisms.

Normal skeletal muscle is known to have strong MT interactions as well (17–19), presumably related to the high concentration of hydrophilic protein macromolecules. Recent investigations have found detectable changes of MT in skeletal muscles after exercise, reflecting shifts in cellular water and changes in intermolecular interactions association with exercise (19). Another recent study characterized the MT changes occurring in rat skeletal muscles associated

with iatrogenically induced myonecrosis (37). MT imaging may also have some application in typifying skeletal muscle neoplasms (38).

The results of this investigation suggest that off-resonance saturation pulse imaging may provide a noninvasive means to characterize the microstructural changes of the diseased extraocular muscles in TRO, as indicated by reduced off-resonance saturation. Furthermore, our results suggest that contrast between normal and abnormal extraocular muscle tissues is improved as the off-resonance pulse is brought closer to water resonance, suggesting a potential role of near-resonance spin-lock imaging in examining these patients. However, MT contrast also differed significantly between healthy subjects and patients with TRO. The optimal saturation effect, MT or spin lock, for achieving contrast of the extraocular muscles may vary at different stages of the disease.

At this point, it is unclear which microstructural changes occurring in the extraocular muscles of TRO patients accounts for the abnormally low spin lock and MT suppression observed in this investigation. The accumulation of fatty tissue may be one contributing factor, because fat is insensitive to the effects of MT and near-resonance spin-lock excitation (above 500 Hz frequency offset) (5, 6, 17). By detecting fatty infiltration, off-resonance saturation imaging could potentially temporally delineate the point at which irreversible structural changes occur within individual extraocular muscles and the point at which steroid and orbital radiation treatments are no longer likely to be effective. The extent to which near-resonance saturation contrast reflects inflammatory cell infiltrates, mucopolysaccharide accumulation, and/or fibrosis within the extraocular muscles is currently unknown. Ultimately, longitudinal and correlative studies are necessary to determine the effects of different histologic phases within the extraocular muscles on near-resonance spin lock and MT contrast throughout the course of the disease.

Off-resonance saturation imaging, particularly spin-lock imaging, may provide new information that is not reflected either in extraocular size or MR signal. The results of this study indicate that simple measurements of extraocular muscle MR signal on T1-weighted images as an indication of fatty infiltration is less differentiating than near-resonance saturation contrast. The combined presence of fatty infiltration increasing signal and adjacent fibrosis decreasing signal on T1-weighted images within a single voxel could average to make each type of muscle tissue change less apparent in some cases. Thus, near-resonance saturation imaging may be superior to signal measurements in detecting these changes. Alternatively, other structural changes in the extraocular muscles in addition to fatty infiltration may account for the abnormally low near-resonance suppression observed in this investigation.

Conclusion

As shown in our study, muscles of normal size and normal signal may have abnormal spin lock and MT contrast, while muscles of large size may show relatively preserved saturation effects. One of our volunteers had preserved saturation in enlarged extraocular muscles, which may have been due to the presence of fibrosis. The abnormal spin lock and MT suppression observed in our one patient who was euthyroid with muscles of normal size and signal suggest that these techniques can characterize microstructural changes in the muscle, unrelated to the presence of elevated thyroid hormone or muscle enlargement. Thus, near-resonance spin-lock and MT imaging may reflect structural changes in the extraocular muscles of Graves' patients, yielding information unobtainable by simple morphologic or MR signal analysis. More research is needed to determine optimal pulse parameters and relative contributions of MT and near-resonance spin-lock contrast in patients at various stages of the disease. Refinements in technique are needed to reduce imaging time and eye motion effects while preserving contrast between orbital fat and extraocular muscles. Studies should be designed to correlate disease duration and various treatments with off-resonance saturation imaging.

References

1. Solomon PH, Chopra IJ, Chopra UC, Smith FJ. **Identification of subgroups of euthyroid Graves' ophthalmopathy.** *N Engl J Med* 1977;296:181–185
2. Caldwell G, Gow SM, Sweeting VM, et al. **A new strategy for thyroid function testing.** *Lancet* 1985;1:1117–1119
3. Char DH. *Thyroid Eye Disease.* 2nd ed. New York: Churchill Livingstone; 1990
4. Wolff SD, Balaban RS. **Magnetization transfer contrast and tissue water proton relaxation in vivo.** *Magn Reson Med* 1989;10:135–144
5. Moran PR, Hamilton CA. **Near-resonance spin-lock contrast.** *Magn Reson Imaging* 1995;13:837–846
6. Ulmer JL, Mathews VP, Hamilton CA, Elster AD, Moran PR. **Magnetization transfer or spin-lock? An investigation of off-resonance saturation pulse imaging using varying frequency offsets.** *AJNR Am J Neuroradiol* 1996;17:805–819
7. Kurki T, Lundbom N, Hannu K, Valtonen S. **MR classification of brain gliomas: value of magnetization transfer and conventional imaging.** *Magn Reson Imaging* 1995;13:501–511
8. Yousem DM, Montone KT, Sheppard LM, Rao VM, Weinstein GS, Hayden RE. **Head and neck neoplasms: magnetization transfer analysis.** *Radiology* 1994;192:703–707
9. Lexa FJ, Grossman RI, Rosenquist AC. **Wallerian degeneration in the feline visual system: characterization by magnetization transfer rate with histopathological correlation.** *AJNR Am J Neuroradiol* 1994;15:201–212
10. Gass A, Barker GJ, Kidd D, et al. **Correlation of magnetization transfer ratio with clinical disability in multiple sclerosis.** *Ann Neurol* 1994;36:62–67
11. Loevner LA, Grossman RI, Cohen JA, Lexa FJ, Kessler D, Kolson DL. **Microscopic disease in normal-appearing white matter on conventional MR images in patients with multiple sclerosis: assessment with magnetization-transfer measurements.** *Radiology* 1995;196:511–515
12. Tomiak MM, Rosenblum JD, Prager JM, Metz CE. **Magnetization transfer: a potential method to determine the age of multiple sclerosis lesions.** *AJNR Am J Neuroradiol* 1994;15:1569–1574
13. Elster AD, Mathews VP, King JC, Hamilton C. **Improved detection of gadolinium enhancement using magnetization transfer imaging.** *Neuroimaging Clin N Am* 1994;4:185–192
14. Finelli DA, Hurst GC, Gullapali RP, Bellon EM. **Improved contrast of enhancing brain lesions on post gadolinium, T1-weighted spin-echo images with use of magnetization transfer.** *Radiology* 1994;190:553–559

15. Mathews VP, King JC, Elster AD, Hamilton CA. **Cerebral infarction: effects of dose and magnetization transfer saturation at gadolinium-enhanced MR imaging.** *Radiology* 1994;190:547–552
16. Mathews VP, Elster AD, King JC, Ulmer JL, Hamilton CA, Strottman JM. **Combined effects of magnetization transfer and gadolinium in cranial MR imaging and MR angiography.** *AJR Am J Roentgenol* 1995;164:169–172
17. Elster AD, King JC, Mathews VP, Hamilton CA. **Cranial tissues: appearance at gadolinium-enhanced and nonenhanced MR imaging with magnetization transfer contrast.** *Radiology* 1994;190:541–546
18. Yousem DM, Suhnall MD, Dougherty L, Weinstein GS, Hayden RE. **Magnetization transfer imaging of the head and neck: normative data.** *AJNR Am J Neuroradiol* 1994;5:1117–1121
19. Yoshioka H, Takahashi H, Anno I, Niitsu M, Itai Y. **Acute change of exercised muscle using magnetization transfer contrast MR imaging.** *Magn Reson Imaging* 1994;12:991–997
20. Bottomley PA, Foster TH, Argersinger RE, Pfeifer LM. **A review of normal tissue hydrogen NMR relaxation times and relaxation mechanisms from 1–1000 MHz: dependence on tissue type, NMR frequency, temperature, excision and age.** *Med Phys* 1984;11:425–448
21. Spencer WH. *Ophthalmic Pathology: An Atlas and Textbook.* 3rd ed. Philadelphia: Saunders; 1986
22. Hufnagel TJ, Hickey WF, Cobbs WH, Jakobiec FA, Iwamoto T, Eagle PC. **Immunohistochemical and ultrastructural studies on the exenterated orbital tissues of a patient with Graves' disease.** *Ophthalmology* 1984;91:1411–1419
23. Fells P, Kousoulides L, Pappa A, Murro P, Lawson J. **Extraocular muscle problems in thyroid eye disease.** *Eye* 1994;8:497–505
24. Willinsky RA, Arensen AM, Hurwitz JJ, Szalai J. **Ultrasonic B-scan measurement of the extraocular muscles in Graves' orbitopathy.** *J Can Assoc Radiol* 1984;35:171–173
25. Nugent RA, Belkin RI, Neigel JM, et al. **Graves' orbitopathy: correlation of CT and clinical findings.** *Radiology* 1990;177:657–682
26. Holt JE, O'Connor PS, Douglas JP, Byrne B. **Extraocular muscle size comparison using standardized A-scan echography and computerized tomography scan measurements.** *Ophthalmology* 1985;92:1351–1355
27. Just M, Kahaly G, Higer HP, et al. **Graves' ophthalmopathy: role of MR imaging in radiation therapy.** *Radiology* 1991;179:187–190
28. Hoh HB, Laitt RD, Wakeley C, et al. **The STIR sequence MRI in the assessment of extraocular muscles in thyroid eye disease.** *Eye* 1994;8:506–510
29. Laitt RD, Hoh B, Wakeley C, et al. **The value of the short tau inversion recovery sequence in magnetic resonance imaging of thyroid eye disease.** *Br J Radiol* 1994;67:244–247
30. Hiromatzu Y, Kojima K, Ishisaka N, et al. **Role of magnetic resonance imaging in thyroid-associated ophthalmopathy: its predictive value for therapeutic outcome of immunosuppressive therapy.** *Thyroid* 1992;2:299–305
31. Hua J, Hurst GC. **Analysis of on- and off-resonance magnetization transfer techniques.** *J Magn Reson Imaging* 1995;5:113–120
32. Henkelman RM, Huang X, Xiang Q, Stanisz GJ, Swanson SD, Bronskill MJ. **Quantitative interpretation of magnetization transfer.** *Magn Reson Med* 1993;29:759–766
33. Hajnal VJ, Baudouin CJ, Oatridge A, Young IR, Bydder GM. **Design and implementation of magnetization transfer pulse sequences for clinical use.** *J Comput Assist Tomogr* 1992;16:7–18
34. Santyr GE, Henkelman RM, Bronskill MJ. **Spin locking for magnetic resonance imaging with application to human breast.** *Magn Reson Med* 1989;12:25–37
35. Santyr GE, Fairbanks EJ, Kelcz F, Sorenson JA. **Off-resonance spin locking for MR imaging.** *Magn Reson Med* 1994;32:43–51
36. Sepponen RE, Pohjonen JA, Sipponen JT, et al. **A method for $T1_\rho$ imaging.** *J Comput Assist Tomogr* 1985;9:1007–1011
37. Mattila KT, Lukka R, Hurme T, Komu M, Alanen A, Kalimo H. **Magnetic resonance imaging and magnetization transfer in experimental myonecrosis in the rat.** *Magn Reson Med* 1995;33:185–192
38. Li KCP, Hopkins KL, Moore SG, et al. **Magnetization transfer contrast MRI of musculoskeletal neoplasms.** *Skeletal Radiol* 1995;24:21–25